PCCP

Accepted Manuscript

ROYAL SOCIETY OF CHEMISTRY

www.rsc.org/pccp

Asymmetric Bifurcated Halogen Bonds

Martin Novák[a,b], Cina Foroutan-Nejad[a,b]* and Radek Marek[a,b,c]*

[a] *CEITEC – Central European Institute of Technology, Masaryk University, Kamenice 5/A4, CZ-625 00, Brno, Czech Republic*

[b] *National Center for Biomolecular Research, Faculty of Science, Masaryk University, Kamenice 5, CZ-625 00 Brno, Czech Republic*

[c] *Department of Chemistry, Faculty of Science, Masaryk University, Kamenice 5, CZ-625 00 Brno, Czech Republic*

* To whom correspondence should be addressed: C. Foroutan-Nejad: 119499@mail.muni.cz, R. Marek: radek.marek@ceitec.muni.cz

Abstract

Halogen bonding (XB) is being extensively explored for its potential use in advanced materials and drug design. Despite a significant progress in describing this interaction by theoretical and experimental methods, the chemical nature remains somewhat elusive and, it seems to vary with selected system. In this work we present a detailed DFT analysis of three-center asymmetric halogen bond (XB) formed between dihalogen molecules and variously 4-substituted 1,2-dimethoxybenzene. The energy decomposition, orbital, and electron density analyses suggest that the contribution of electrostatic stabilization is comparable with that of non-electrostatic factors. Both terms increase parallel with increasing the negative charge of the electron donor molecule in our model systems. Depending on the orientation of the dihalogen molecules, this bifurcated interaction may be classified as 'σ-hole – lone pair' or 'σ-hole – π' halogen bonds. Arrangement of the XB investigated here deviates significantly from a recent IUPAC definition of XB and, in analogy to the hydrogen bonding, term *bifurcated halogen bond* (BXB) seems to be appropriate for this type of interaction.

Graphical abstract

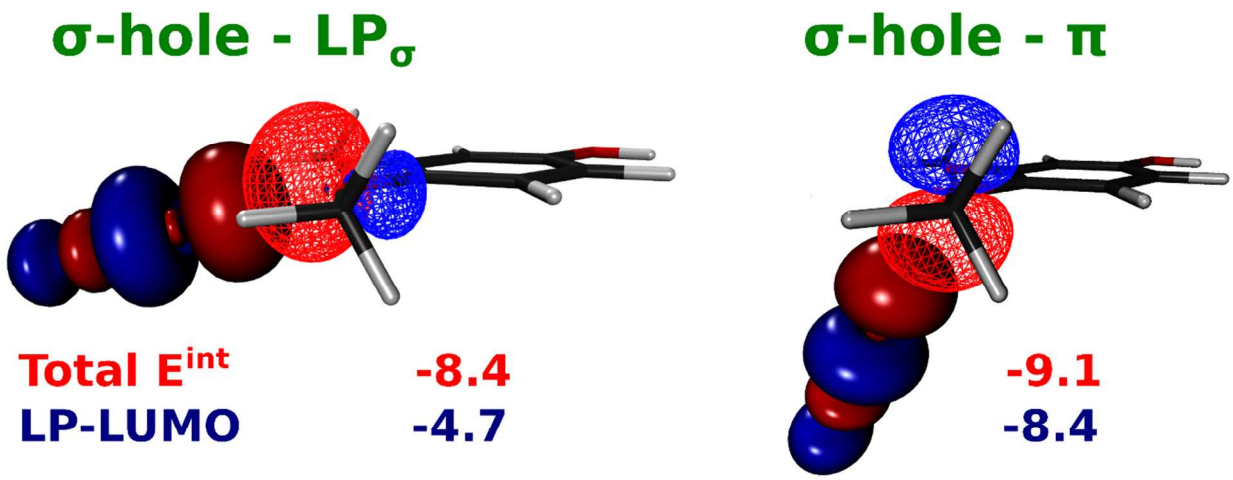

1 INTRODUCTION

Non-covalent interactions have been of a tremendous interest in both basic and applied research for many decades.[1] In recent years, halogen bonding (XB) has drawn attention of many researchers because of its directionality and tunability.[2–6] Diversity of halogenated biological molecules suggests that XBs might play an important role in cellular structures. This topic has recently been reviewed by Wilcken and coworkers.[7] XBs are also widely used in supramolecular chemistry and crystal engineering for designing novel functional materials.[8–14]

XBs form as a result of anisotropic electron distribution of halogen atoms upon its bonding with electron-withdrawing moieties (-Z), which can be of either organic or inorganic nature. This arrangement results in a formation of specific region of positive electrostatic potential located at the outer tip of the halogen, sometimes called a σ-hole,[5,15–20] whereas the electrostatic potential on the rest of atomic surface of the halogen remains negative. In special cases, when halogen is attached to strongest electron withdrawing moieties, its whole surface can be positive.[21] In general, a single halogen atom can interact in some directions as an electron donor and in other directions as an electron acceptor. The angle formed between three atoms Z-X···B, where B is a Lewis base, should be close to 180°. In contrast, the angle for Z-X···A arrangement, where A is a Lewis acid, should be around 120° (Figure 1).[22] The σ-hole interactions have been investigated and visualized using the electrostatic potential maps,[23,24] Laplacian of electron density,[25,26] and natural orbital for chemical valence (NOCV).[27]

It has been found that the magnitude of the σ-hole depends not only on the electronegativity of the electron withdrawing substituent (Z) but also on its ability to accumulate electrons (charge capacity).[23] The anisotropy of the electrostatic potential originates in a depletion of electrons from the outer lobe of the *p* orbital of the halogen, which is involved in a covalent bonding with Z.[18]

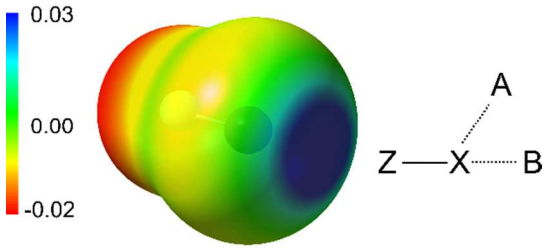

Figure 1: The electrostatic potential of BrF mapped on the molecular surface (isosurface of 0.001 a.u.) showing the σ-hole.[18] Scale in atomic units. Halogen-containing compound Z-X can interact with both

the Lewis acid A – with the Z-X···A angle around 120° - or the Lewis base B – with the Z-X···B angle around 180°.

In general, three factors determine the σ-hole presence or absence and its magnitude[28]: a) the electronegativity of the halogen atom, b) its polarizability, and c) the electron-withdrawing power and capacity of Z in Z-X molecule. It should be mentioned that the presence of a true positive region at the halogen-bond donor is not required as the charge density can be polarized in the interacting system resulting from the formation of regions of the charge depletion and charge accumulation on the XB donor and acceptor (a hole-lump interaction).[29]

The nature of interaction responsible for the formation of XB is frequently assigned to be electrostatic with magnitude of electrostatic stabilization being dependent on the size of the σ-hole.[3–5,26,30–33] Besides, NBO analysis[34] revealed that XB complexes have some charge transfer from the electron donor to the antibonding orbitals of halogenated electron acceptors.[30,35] In addition, dispersion interaction, i.e. exchange-correlation, can be the dominant stabilizing factor in some cases.[17,36,37] The similarity between the resonance assistance of guanine quartets with the halogenated analogues proved that the charge transfer is a significant contributor to the total interaction energy for XBs in these systems.[38] The results reported by Riley and Hobza indicate that for the XB between fluorinated halomethane and formaldehyde the role of electrostatic interaction increases with the number of fluorine atoms attached to the halomethane.[37] In spite of successful application of *ab initio* and DFT methods, classical empirical force-fields with partial charges localized on nuclei cannot account for the anisotropy of the electron distribution in XB systems. However, attempts for a more rigorous description of this phenomenon in molecular mechanics are under way.[39–41] It is worth noting that the σ-hole bonding is not limited to halogens, in fact, elements from groups 14 to 16 can also participate in this type of interaction.[42–46]

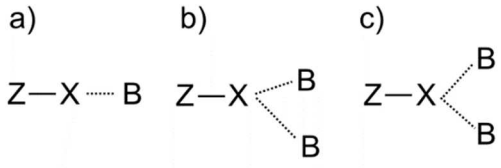

Figure 2: Three different arrangements of XB: a) two-center XB with single Lewis base as electron donor; b) bifurcated asymmetric XB where the distance to one Lewis base is shorter than to the other one; c) bifurcated symmetric XB where both XB distances are equal.

Three possible arrangements of XB with one or two electron donors are shown in Figure 2. Most studies focused on the XB acceptors with a single electron-rich center (two-center XB); indeed, complexes with two electron-rich species (three-center XB) are relatively scarce.[11,47,48] This might be due to the fact, that the bifurcated arrangement of the XBs appears to be disfavored in comparison with the two-center XBs.[47] Thus, in the present paper we exploit the nature of bonding in complexes of dihalogen molecules BrF, BrCl, and ClF bound to two oxygen atoms (forming a three-center, bifurcated halogen bond - BXB) of *ortho*-dimethoxybenzene molecule variously substituted (electron donating/withdrawing moieties) at 4-position of the 1,2-dimethoxy benzene ring by DFT methods. Halogen bonding in our model systems is studied using a wide variety of orbital- and density-based probes to scrutinize the very nature of halogen bonds. We intentionally selected various approaches to realize if the picture of bonding remains the same in different perspectives from orbital- to density-based approaches.

2 METHODS

The geometry optimization was performed using Gaussian 09, Revision A.02[49] program suite. Because of the extended number of model complexes the density functional theory was chosen for its balanced tradeoff between accuracy and computational cost. We selected M06-2X hybrid functional, developed by Truhlar and coworkers,[50] for its superior performance compared with the "golden standard" CCSD(T) method in halogen-bonded complexes in terms of geometry and energy.[51] Large def2-TZVPPD[52] triple-ζ basis set equipped with two sets of polarization and diffusion functions was used for the description of all atoms. "Tight" convergence criteria were set during the optimization procedure. According to the Hessian matrix eigenvalues, all reported complexes were assigned to be true local minima on their potential energy surface. The interaction energies (ΔE^{Int}) are reported as the differences between the electronic energies of complexes and their respective monomers in geometries as they appear in the complexes, Equation (1).

$$\Delta E^{Int} = E^{opt}_{complex} - \sum E_{monomers} \qquad (1)$$

Therefore, the reported values do not include the deformation energies required to change the optimized monomers into their geometries in the complexes.

NBO analysis[34] was performed using NBO 3.1[53] as implemented in Gaussian 09 package. Electron deformation density (EDD) maps were produced using Gaussian 09 checkpoint files and a locally developed workflow.[54,55] The procedure is based on subtraction of electron densities of the species of interest, Equation (2):

$$\Delta\rho(r) = \rho(r) - \sum_{N} \rho_N(r) \qquad (2)$$

ADF (version 2013.01c)[56] suite of programs was used for performing the Energy Decomposition Analysis (EDA)[57] and Natural Orbital for Chemical Valence (NOCV).[58,59] TZ2P Slater type basis set was used to describe the electronic structure of complexes. The usual energy contributions for EDA that are of great interest to chemists are defined as follows, Equation (3):

$$\Delta E^{Int} = \Delta E^{Pauli} + \Delta E^{Elstat} + \Delta E^{Orbital} \qquad (3)$$

where ΔE^{Int} is the total interaction energy, ΔE^{Pauli} is the Pauli repulsion (exchange-repulsion) term as defined in ADF package, ΔE^{Elstat} is the electrostatic term, and $\Delta E^{Orbital}$ is the orbital contribution to the total energy. However, an alternative decomposition can be based on the contributions of physical factors in EDA, namely, electrostatic energy (ΔE^{Elstat} + $\Delta E^{Coulomb}$), kinetic energy (ΔE^{Kin}), and exchange-correlation (ΔE^{XC}). Here, we considered both approaches as implemented in ADF.

The Quantum Theory of "Atoms in Molecules", QTAIM,[60] analysis was carried out using AIMAll[61] software on the wavefunctions produced during optimization (at M06-2X/def2-TZVPPD computational level).

3 RESULTS AND DISCUSSION

In this work complexes between three dihalogen molecules (ClF, BrF, and BrCl) and a wide range of 4-substituted 1,2-dimethoxy benzenes with various XB-acceptor properties were selected. In the studied complexes, always less electronegative atom of the dihalogen molecule interacts with electron donor, i.e., Cl in ClF and Br in BrF and BrCl molecules. Two methoxy groups of variously 4-substituted 1,2-dimethoxybenzenes (see Figure 3) serve as electron donor sites; therefore, all the selected systems bear two non-equivalent methoxy groups (for R = H, two methoxy groups are

identical). The full list of substituents is as the following:

I) Negatively charged: COO^-, O^-, PO_3H^-, S^-, SO_2^-, SO_3^-

II) Neutral: Br, C_2H_3, CF_3, CH_3, CHO, Cl, CN, COOH, F, H, NH_2, NO_2, OCH_3, OCHO, OH, SCH_3, SH, SO_2Cl, SO_3H

III) Positively charged: $CH_2NH_3^+$, $N(CH_3)_3^+$, NH_3^+, $S(CH_3)_2^+$

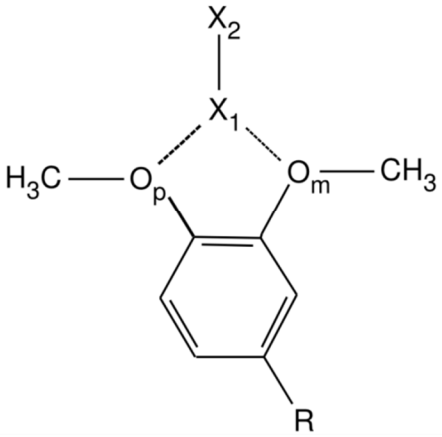

Figure 3: Schematic drawing of complexes studied in this work. R is the variable substituent, O_m and O_p represent the oxygens (methoxy groups) in meta- and para- positions (relative to R), respectively. X_1-X_2 is the XB donor molecule. The dashed lines depict the XBs.

Two different geometries for each molecule were studied: first in which the dihalogen is closer to the oxygen atom in *meta*-position, and second in which dihalogen is closer to the oxygen atom in *para*-position with respect to the substituent R. These complexes from now onwards will be referred to as m-R or *meta*-R for X_1-X_2 closer to O_m and p-R or *para*-R for X_1-X_2 closer to O_p. With the single exception (m-$SCH_3\cdots$BrCl complex), minima were located on the potential energy surface for both geometries.

3.1 Characterization of Complexes

Electrostatic Potential and Polarizability of XB Acceptors

The XB has been described as highly directional interaction where the positive region representing the σ-hole points towards the most negative region of the XB acceptor.[4,62] Studying the electrostatic potential maps shows that the most negative region in our selected model XB acceptors is located approximately in-between the two methoxy oxygens, Figure 4a. Therefore, from a simple electrostatic model one may expect a symmetric three-center XB to be formed, i.e., the two X···O

distances should be equal. However, our results as well as those published previously[11,47,48] conclude that the asymmetric interaction is preferred and, the symmetric arrangement is a first-order saddle point. We rationalize this behavior by taking into account the polarizability in different directions.[63] Inducing a shift of electron density by a positive point charge (+ 0.5 a.u) placed roughly at the position where the halogen nucleus is expected to be located in the complex (in the plane of aromatic system, 3 Å from both oxygens), we demonstrate the polarizability of different regions at the XB-acceptor site. The electron deformation density (EDD) map,[54,55] Δρ, generated by subtracting the unperturbed electron density from the perturbed one is depicted in Figure 4b. The electron density increases most significantly at the connection between oxygens and the point charge. Clearly, the EDD map presented in Figure 4b resembles those calculated for the interaction of the XB acceptor with BrF molecule (see Section 3.4 for details). This indicates that the polarization effect can be responsible for the asymmetric behavior of the selected systems.

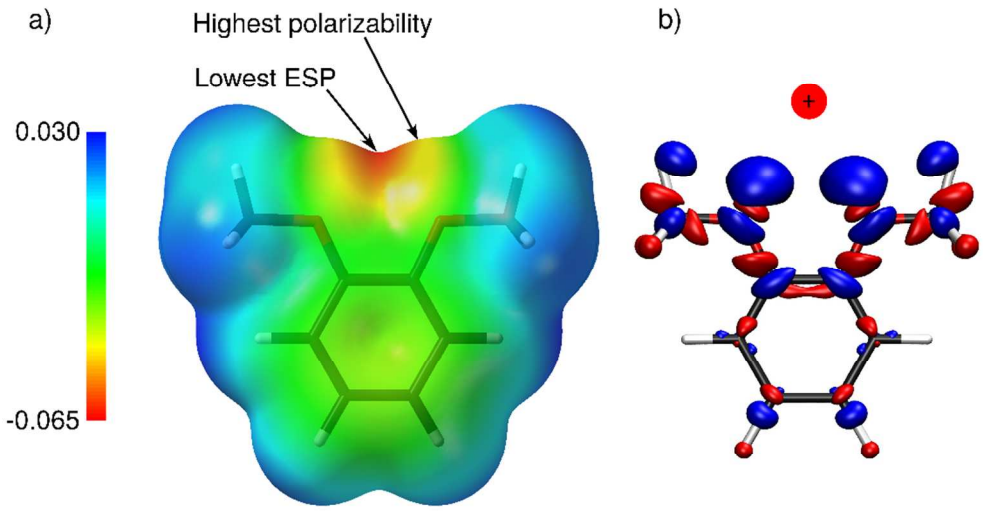

Figure 4: a) Electrostatic potential (ESP) of 1,2-dimethoxybenzene (in a.u.). The region with the most negative ESP is indicated by arrow as well as the region with highest polarizability. b) EDD map generated by subtracting an unperturbed electron density from the electron density perturbed by a + 0.5 a.u. point charge placed in the aromatic plane, 3 Å from the methoxy oxygens. Blue and red lobes represent regions of the electron concentration and electron depletion (isosurface of 0.001 a.u.), respectively.

Geometry and Interaction Energy of Complexes

The interaction energy for the chosen complexes varies in a relatively broad range, approximately

between -3.5 and -21.0 kcal.mol^{-1}. The thermodynamic stabilities of the complexes with respect to the free XB donors follow the expected order of BrCl ≈ ClF < BrF. From the XB-acceptor point of view, the complexes were separated into three major groups according to the formal charge of the R substituent on benzene moiety. The weakest interaction was observed for the positively charged species (-3.5 to -5.0 kcal.mol^{-1}) followed by the neutral ones (-5.0 to -9.0 kcal.mol^{-1}) and the strongest interactions resulted upon substitution of benzene ring by the negatively charged groups (-9.0 to -21.0 kcal.mol^{-1}). This is in line with a very recent data published by Syzgantseva and coworkers[36] where the complexes with negatively charged electron donors showed one order of magnitude higher interaction energies than the neutral ones.

In most cases the optimization resulted in such geometries that the distances between interacting halogen atom and the donor oxygens were smaller than the sum of the van der Waals (vdW) radii for these atoms (see Supporting Information, SI). The angles between the dihalogen molecules and the aromatic rings were measured as the angles between the X_1–X_2 bond and the aromatic plane (the values are listed in SI). Clearly, there is a wide range of X_1–X_2 orientations with respect to the aromatic ring from almost in-plane, for example, m-$SO_2Cl\cdots$BrF complex (angle of only 3.1°, see Figure 5a), up to almost perpendicular arrangement for m-$NH_3^+\cdots$BrCl complex (angle of 86.1°, see Figure 5b). For most of the complexes, both donor methoxy groups (methoxy carbons) remained approximately in plane with the aromatic ring. Our calculations show that multiple local minima can be found at least for some of the considered complexes, see Section 3.3 for examples. The potential energy surface is very flat as the barrier between the local minima is approximately 0.5 kcal.mol^{-1}. It should be noted that for the same type of complexes the ΔE^{Int} is slightly more negative for higher angle values.

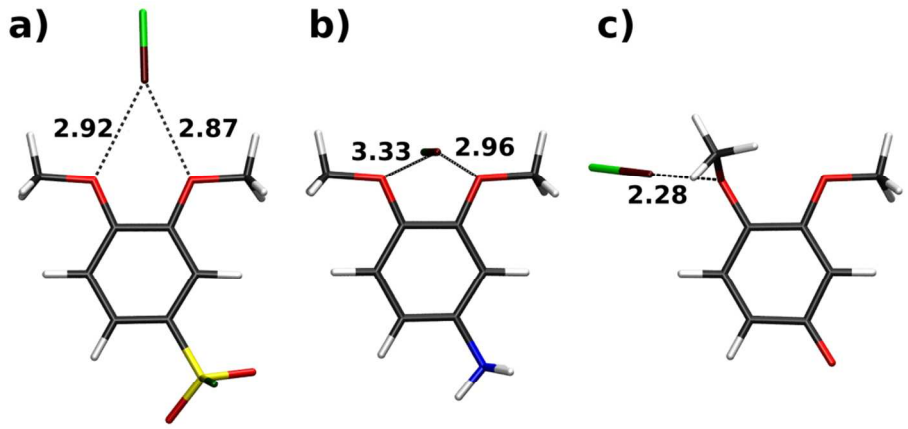

Figure 5: Three selected examples of extreme geometries. a) m-$SO_2Cl\cdots BrF$ complex, where the dihalogen molecule lies almost in the plane of aromatic ring. b) m-$NH_3^+\cdots BrCl$ complex, where the dihalogen molecule is placed perpendicularly with respect to the aromatic plane. c) p-$O^-\cdots BrF$ complex in which the bromine is bound only to the methoxy group (two-center XB) in para- position with respect to the substituent, where the methoxy group is turned out-of-the-plane of the aromatic ring already in the isolated XB acceptor. Distances are presented in Å.

BrF and ClF molecules form merely two-center XB complexes with O^- substituted benzene derivatives in para- position (see Figure 5c). The reason behind this behavior is that the para- methoxy group is turned out-of-plane in the XB-acceptor and its lone pairs point to such direction that it would be energetically unfavorable for the dihalogen to form bifurcated XB bond. It is worth mentioning that these two complexes are among the most stable complexes studied in this work. The strength of the XBs is also pronounced in very short contacts between the interacting species, only 68 % of the sum of the vdW radii (strong XB) whereas for the other complexes the contacts are approximately 90% of the sum of vdW radii (medium to weak XB).[62]

At this point it should be emphasized, that the variations in interaction energies between *meta*- and *para*- complexes with the same XB-acceptor are generally very small.

3.2 Quantum Theory of Atoms in Molecules (QTAIM)

Quantum Theory of "Atoms in Molecules", QTAIM, introduced by Bader is one of the most widely used methods for analyzing the electron density in molecular and supramolecular systems. The central advantage of QTAIM is that it is intimately related to the physical observables, i.e., the electron

density and its derivatives.

Line Critical Points*[64] *(LCP) and Delocalization Indices (DI) between XB Donor and Acceptor Atoms

Properties of Line Critical Points (LCPs), or (3,-1) critical points, have been used extensively for assessing bonding properties. It should be recalled that there is no direct link between presence/absence of LCPs and chemical bond, however, LCP properties, besides other bonding descriptors, i.e. integration properties, may be used to characterize bonding pattern in a system.[52] With a few exceptions, two LCPs were found between the XB donor halogen atom and the electron-donating oxygens (for example, see Figure 6). The selected quantities (electron density, Laplacian of the electron density, and the energy density) for these LCPs of all complexes are reported in Supporting Information along with the delocalization indices (DI) between the halogen and both oxygen atoms.

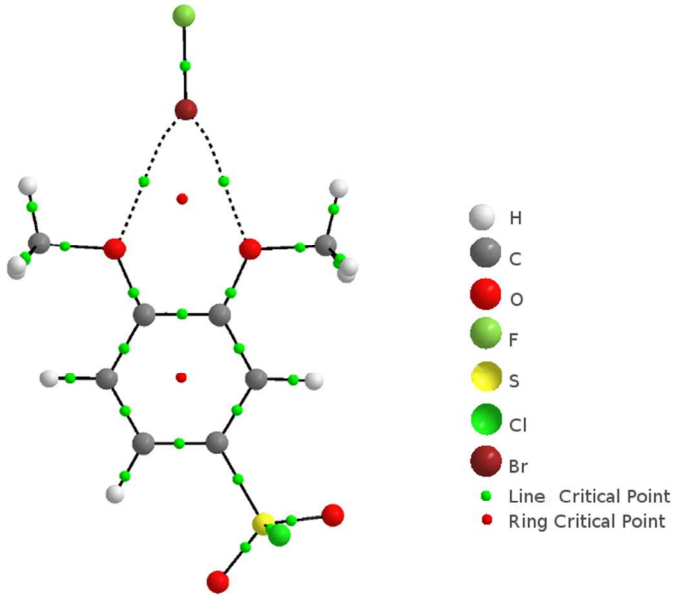

Figure 6: m-$SO_2Cl\cdots BrF$ complex showing all the line paths with LCPs and rings with Ring Critical Points (RCPs).

The LCP electron densities are relatively small, usually around 0.02 and 0.01 a.u. for the shorter and longer X···O distances, respectively. The electron density at LCP is higher for the negatively charged substituents on the benzene moiety as compared with the neutral and positive substituents. For all three dihalogen molecules good linear correlations between the interaction energies and the sum of the electron densities calculated for the corresponding LCPs were found. These correlations are shown in Figure 7.

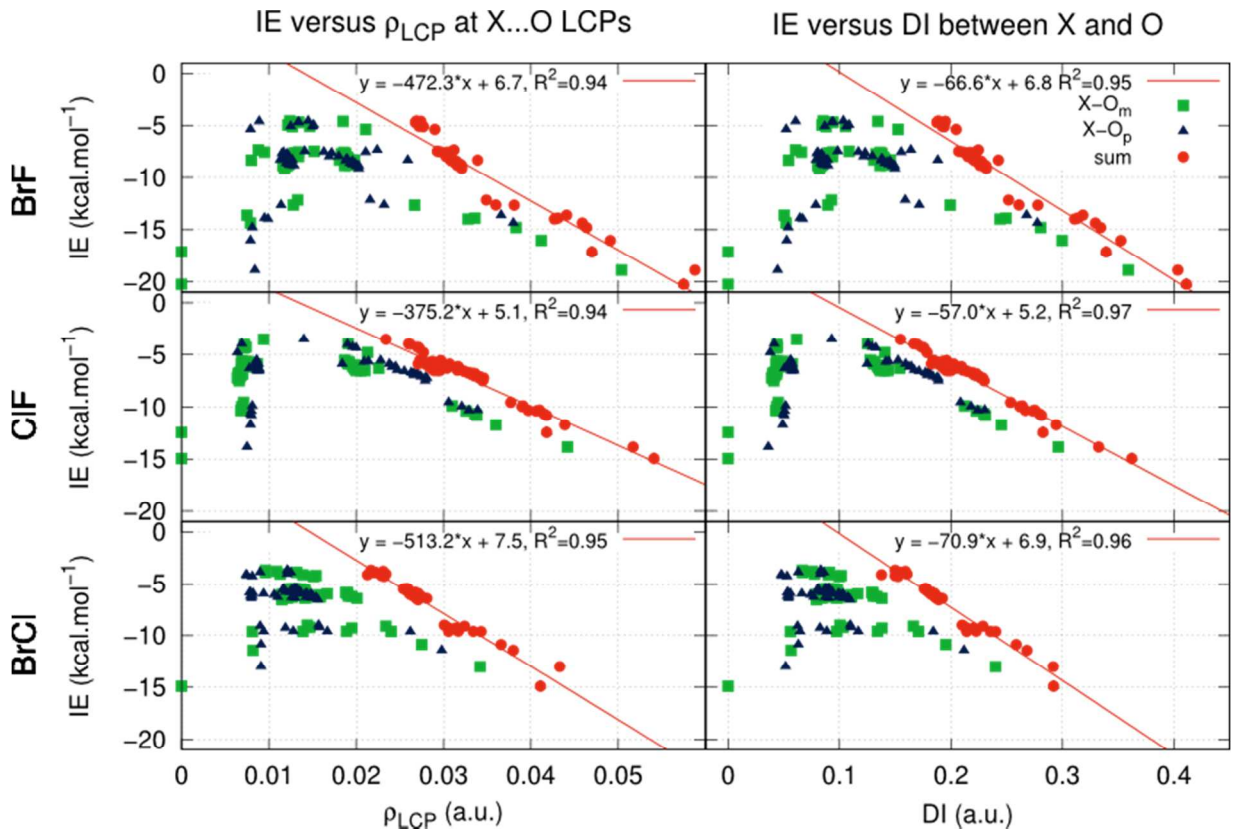

Figure 7: Left: Interaction energies versus electron densities of LCPs between the halogen and oxygen atoms. Right: Interaction energies versus delocalization indices between halogen and oxygen atoms. The linear regression functions along with R^2 coefficients are given for each dataset. Green squares and blue triangles represent respective contributions from X-O_m and X-O_p contributions, red circles are the sums of these two contributions.

The values of the Laplacian of the electron density at LCPs are small and positive. From the point of view of the orthodox QTAIM all interactions are closed shell. On the other hand, the energy density is small and negative for 15 negatively charged complexes and small and positive for the rest of systems; small values of the energy density at LCP is another sign of the closed shell interaction.

Delocalization index, DI, is an integration property, which is useful for characterizing the chemical bonds. DI can be defined between any pair of atoms, irrespective to the fact that (3, -1) CP is present or absent between that couple. In fact, the DI quantifies the extent of the electron exchange between any atomic pair that is a direct measure of covalence.[65,66] Recent studies demonstrate that DI correlates well with contribution of the exchange-correlation energy within the framework of the theory of Interacting Quantum Atoms (IQA).[67,68]

Our QTAIM calculations show that the interaction energies correlate linearly with the sum of the delocalization indices between the halogen and the two oxygen atoms (Figure 7). As expected, the higher the degree of exchange, the stronger the halogen bond is. Although this linear correlation does not provide any clue about the magnitude of the contribution of exchange-correlation in binding energy, it implies that the contribution of this term is a constant part of the total binding energy.

LCPs and DIs between Oxygens and Aromatic Carbons

Our studies suggest that XB interaction energies can be related to, or predicted from, the properties of oxygen-aromatic carbon bond (O–C_{arom}) either. In fact, there is an interesting dependence between the XB binding energy and the electron density at the LCP of the O-C_{arom} bond for the *monomeric* XB acceptor, see Figure 8. In addition, electron delocalization between this O-C_{arom} atomic pair changes upon complexation. As shown in Figure 8, sum of O–C_{arom} DIs (for isolated XB acceptor) can be related to the XB interaction energy.

The sums of the electron densities for O–C_{arom} LCPs are largest for the positively charged substituents and they decrease in parallel with decreasing the formal charge of the substituent. The same trend is observed for the sums of DIs. This can be rationalized by considering a donation of the electrons from the lone electron pairs of the oxygen atoms into the electron-poor benzene moiety once a positively charged substituent is attached to the ring. On the other hand, with an electron-donating substituent the electron-donation from the lone pairs of oxygen atoms in methoxy groups to the benzene moiety is less efficient. This leads to a lower electron density at the O-C_{arom} LCP. Consequently, more electrons at the oxygen LPs are available for interaction with the dihalogen molecules. The numbers are also supported by the $\nabla^2\rho$(O-C_{arom}), which are more negative for the positively charged complexes indicating higher charge concentration in between these nuclei (see Supporting Information).

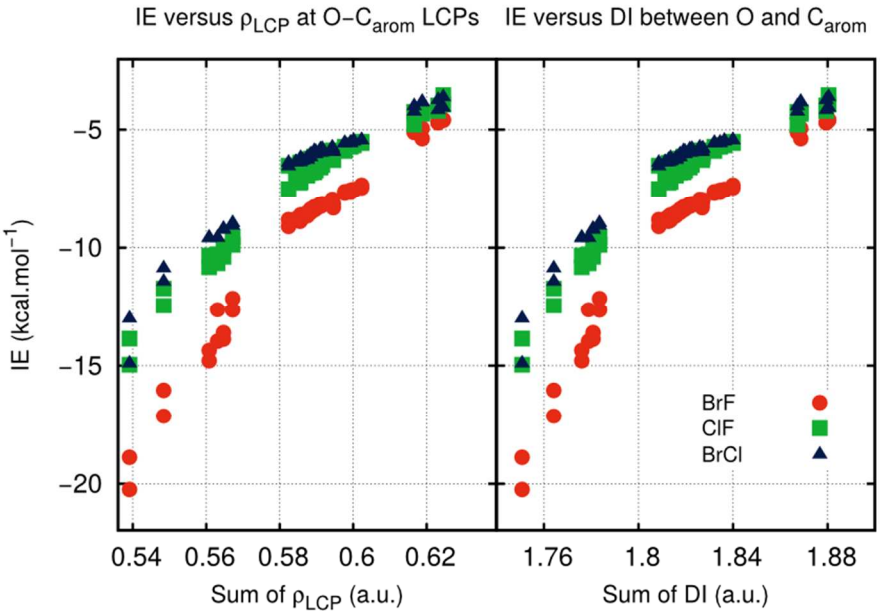

Figure 8: Relations between – Left: the sum of the electron densities at O-C_{arom} LCPs and the interaction energies for all optimized complexes. Right: sum of delocalization indices between O and C_{arom} atoms versus the interaction energies. The electron densities and delocalization indices are extracted from calculations on the isolated XB acceptors.

3.3 Energy Decomposition Analysis (EDA)

The interaction energies were calculated using geometries obtained from M06-2X/def2-TZVPPD optimization. To unveil contributions of various factors in the interaction energy, EDA analysis[69] (Ziegler-Rauk method)[70] using M06-2X functional and TZ2P Slater-type basis set was performed by ADF package.[56] Two XB-acceptor molecules from each group of complexes bearing negative, neutral, and positive substituents were selected (see Table S14 and S15) and two minima for each meta- and para- complex were considered. One with the dihalogen molecule oriented more 'in plane' and another with the dihalogen closer to the 'perpendicular' position. Only one local minimum was found for m-$COO^{-}\cdots$BrF, p-$COO^{-}\cdots$BrF, and m-$N(CH_3)_3^{+}\cdots$BrF complexes.

Individual contributions to the interaction energy (ΔE^{Int}) coming from exchange-correlation (ΔE^{XC}), kinetic (ΔE^{Kin}), Coulomb ($\Delta E^{Coulomb}$), and electrostatic (ΔE^{Elstat}) terms are summarized in Table S14. Inspecting the energy components by plotting the exchange-correlation contribution (ΔE^{XC}) versus the sum of the electrostatic terms ($\Delta E^{Elstat} + \Delta E^{Coulomb}$) in the interaction energy reveals an interesting

trend. Based on Figure 9a (and Table S14), the main stabilizing factor for the weak halogen bonds (benzenes bearing electron-withdrawing groups) is the exchange-correlation term. However, for the strongly bonded complexes, the contribution of the electrostatic forces in the bonding increases dramatically and becomes the major factor in the interaction energy. It is important to highlight that there is a linear correlation between the contribution of exchange-correlation (ΔE^{XC}) and that of electrostatic forces ($\Delta E^{Elstat} + \Delta E^{Coulomb}$) in the interaction energy (see Figure 9a).

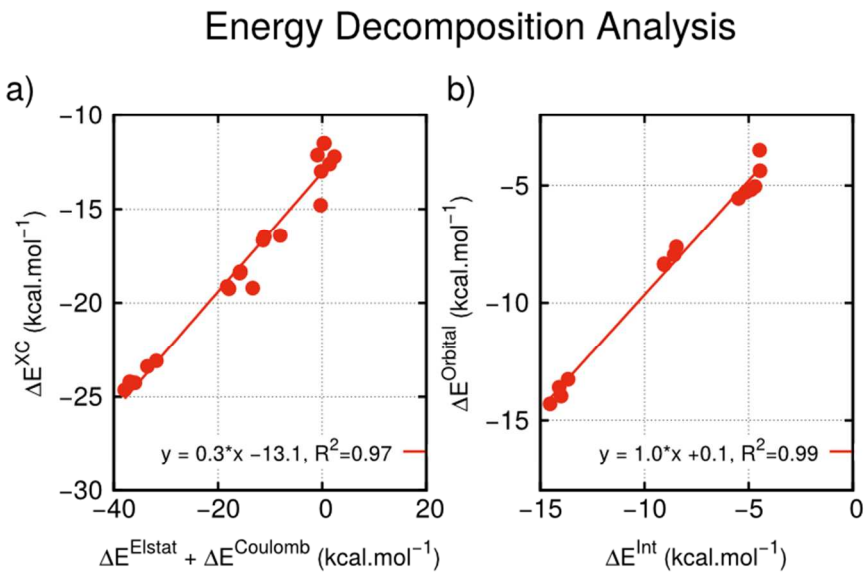

Figure 9: Energy decomposition analysis of total M06-2X/TZ2P interaction energies for BrF complexes. **a)** Exchange-correlation stabilization energy against the sum of electrostatic and Coulomb part of interaction energy extracted from the EDA analysis. **b)** $\Delta E^{Orbital}$ against ΔE^{Int} for complexes with the orientation of BrF molecule closer to the perpendicular position (> 45°).

García-Revilla and coworkers recently demonstrated[71] that the exchange-correlation energy correlates with the internuclear distance and, with the interaction energy between the two atoms according to IQA analysis.[67,68] Previously, EDA and QTAIM analyses results were shown to be inconsistent;[72] however, in our case both approaches point to the same conclusion. Indeed, our results from the two independent methods, EDA and QTAIM (DIs, Section 3.2) suggest that the "electron sharing" contribution correlates linearly with the total XB interaction energy (Table S14).

It should be noted that, based on the standard EDA decomposition scheme using Equation (3), orbital part ($\Delta E^{Orbital}$) counts for a constant portion of the total interaction energy in the systems with

orientation of the dihalogen closer to the 'perpendicular' position, > 45° (see Figure 9b). In addition, the orbital term increases in parallel with increasing the negative charge of the complex. However, contributions of individual terms in ΔE^{Int} somewhat vary with varying the angle between the dihalogen and the aromatic plane. To analyze electron redistribution and orbital interactions for these arrangements in a more detail, we resorted to the electron deformation density, ETS-NOCV, and NBO methods.

3.4 Electron Deformation Density (EDD)

To obtain an insight towards the redistribution of electron density upon complexation, the EDD maps were generated for three selected BXB complexes: p-$S(CH_3)_2^+$···BrF, p-Br···BrF and p-SO_2^-···BrF (see Figure 10). Maps were obtained by subtracting the electron densities of the monomers in the geometry as they appear in the complexes from the electron density of the complex.

In general, electron density is shifted towards the dihalogen molecule and the scale of the changes increase with the increase of the interaction energies. There is a significant decrease of electron density in the halogen region between Br and O accompanied by the charge concentration in the π-space of the halogen (the blue "toroidal" lobes around the bromine atom in Figure 10). In addition, it is clear that in all cases both donating oxygens supply electrons into the XB thus confirming the bifurcated nature of this interaction. p-$S(CH_3)_2^+$···BrF, for example, is an almost C_s symmetric complex where the Br···O distances are nearly identical and also the EDD lobes on both methoxy groups are very similar. The other two selected complexes are more asymmetric as the contributions of the two oxygens also are. This is consistent with the results of the QTAIM analysis (Section 3.2), where DI contributions of both methoxy groups, irrespective to the presence or absence of LCPs, have to be included in order to obtain linear dependencies. The total charge transfer, computed as the amount of negative charge transferred from electron donor to electron acceptor using natural atomic charges, was determined to increase from the positively charged complexes (0.002 e^-) through the neutral ones (0.010-0.020 e^-) to the negatively charged systems with typical values of 0.050-0.100 e^-.

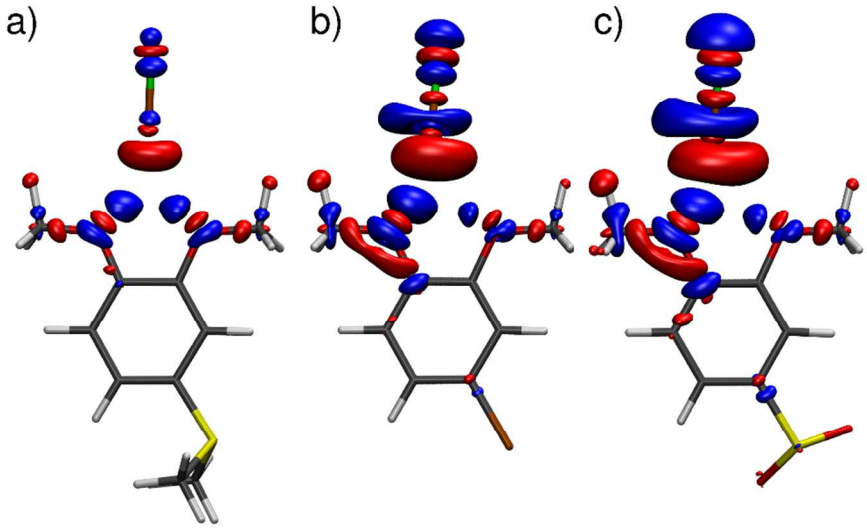

Figure 10: Visualization of electron deformation density (EDD; Blue: charge concentration, red: charge depletion; Isosurfaces at 0.001 a.u.). a) p-$S(CH_3)_2^+\cdots$BrF, b) p-Br$\cdots$BrF, c) p-$SO_2^-\cdots$BrF.

In addition, the NOCV analysis was performed to get a deeper understanding of the EDDs. Since the deformation of electron density is predominantly found in the bonding region, relatively small number of NOCVs will significantly contribute to the total EDD, whereas most of the orbitals do not participate in bonding. The largest contributions to $\Delta\rho$, along with the orbitals which contribute to $\Delta\rho_1$, are visualized in Figure S1 in the SI. The shapes of the orbitals φ_{-1} and φ_1 indicate that they participate in σ-bonding. Only the $\Delta\rho_1$ significantly contributes to the total $\Delta\rho$ while all other channels are much smaller in magnitude (electron exchange between occupied and vacant orbitals, v_k, smaller than 0.1). This is evident from the comparison of $\Delta\rho$ (Figure 10) and $\Delta\rho_1$ (Figure S1) where the shape of $\Delta\rho_1$ NOCV closely resembles the total $\Delta\rho$ in the bonding region. Prevailing red lobes at XB acceptors and blue lobes at XB donors indicate electron transfer towards dihalogen molecules. The eigenvalues v_k increase from 0.11 for p-$S(CH_3)_2^+\cdots$BrF (interaction energy -2.5 kcal.mol^{-1}), to 0.16 for p-Br$\cdots$BrF (interaction energy -4.0 kcal.mol^{-1}), and up to 0.22 for p-$SO_2^-\cdots$BrF (interaction energy -6.5 kcal.mol^{-1}).

3.5 Natural Bonding Orbitals (NBO)

To unveil the contributions of the individual lone pairs of electrons (LPs) at the XB-acceptor oxygen atoms for various orientations of dihalogen molecule, natural bonding orbital (NBO) analysis

was employed. The second-order stabilization energy of interacting orbitals *i* and *j* is computed according to standard NBO approach by Equation (4):

$$E(2) = q_i \frac{F(i,j)^2}{\epsilon_i - \epsilon_j} \qquad (4)$$

where q_i is the occupation number of Lewis-type orbital i, F(i, j) is the off-diagonal Fock matrix element, and ε_i-ε_j is the energy difference between the diagonal elements of the Fock matrix.

In the selected model systems one of the lone pairs on both O_m and O_p is delocalized on the aromatic ring (almost complete p-hybridization, further denoted as "LP_π", Figure 11a) and contribute to its stability with the highest second-order perturbative estimate of approximately 35.0 to 40.0 kcal.mol^{-1}. In other words, it donates electrons into the π^* of the C-C aromatic bond. The magnitude of this stabilization depends on the substituent R and increases in order of negative < neutral < positive, qualitatively supporting the data from the QTAIM analysis, where the highest electron density/DI was observed between the aromatic ring carbons and electron-donating oxygens following the same order (c.f. Figure 8). This value is decreased upon complexation and the LP on the oxygen atom closer to the halogen is affected more (by approximately 4.0 kcal.mol^{-1}) than the other one (approximately 0.5 kcal.mol^{-1}).

The other LP of methoxy oxygen is oriented in plane of the aromatic system pointing outside the molecule and is referred to as "LP_σ". This NLMO (Figure 11b) has s:p ratio of approximately 2:3.

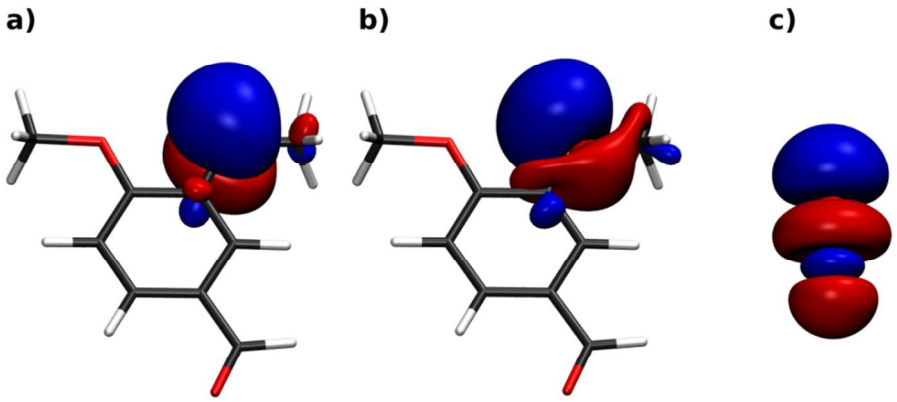

Figure 11: Two NLMOs representing the lone pairs of electrons at O_m in 1,2-dimethoxybenzene-CHO monomer: a) p-hybrid NLMO as extension of the delocalized π-system of the 6-membered ring; b) sp-hybrid NLMO of the second LP on the same oxygen. c) LUMO of the BrF molecule. Isosurfaces at

0.02 a.u.

The most important stabilization from the NBO point of view is the $LP_{Oxygen} \rightarrow LUMO_{dihalogen}(\sigma^*)$ interaction. It is clear that the contributions of respective LPs to the total interaction energy depend on the angle between the dihalogen molecule and the aromatic ring due to "LP-LUMO" overlap, c.f. Figure 11 and Figure 12. Whereas for the lower values of this angle (in-plane position) the main stabilization comes from the sp-hybridized LP_σ, for the high values of the angle (perpendicular position) the stabilization from the p-hybridized LP_π orbital is more important. We suggest to denote the former as σ-hole···LP_σ interaction and the latter as σ-hole···LP_π interaction.

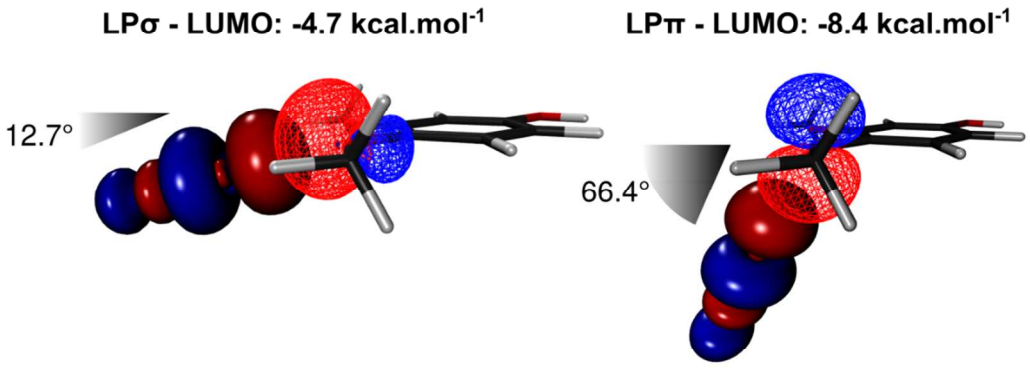

Figure 12: Left: p-OH···BrF complex where the dihalogen lies approximately in the aromatic plane. The highest stabilization (-4.7 kcal.mol^{-1}) originates in the LP_σ–LUMO interaction. Right: p-OH···BrF complex with approximately perpendicular arrangement of the dihalogen with respect to the aromatic plane. In this complex it is LP_π–LUMO interaction with highest second-order perturbative estimate (-8.4 kcal.mol^{-1}). It should be recalled that the total interaction energy is very similar in both cases (-8.4 vs. -9.1 kcal.mol^{-1}). The interacting lone pair of O_p is depicted in wireframe, whereas LUMO of the dihalogen molecules is shown by solid surface. Isosurfaces at 0.02 a.u.

It should be noted that in the system containing O^- substituent, the conjugation of LP_π with the electron-rich aromatic part is very weak (less than 10.0 kcal.mol^{-1}) allowing the rotation of the *para*-methoxy group out of the aromatic plane (even for the isolated XB acceptor).[73] This geometric arrangement enables the accumulation of electron density in the regions of the lone pairs and a stronger interaction with the halogen atom forming a standard, two-center XB (see Supporting Information).

4 CONCLUSIONS

In the present contribution we studied asymmetric bifurcated halogen bonds (BXB) between substituted dimethoxy-benzene donors and dihalogen molecules (FCl, FBr, and ClBr). Studying the relative energies of different conformers demonstrates that the potential energy surface for our model bifurcated halogen-bonded complexes is very shallow. Indeed, small energy differences between the local minima may provide a chance to form dynamic equilibria among various states in the systems. Asymmetry of the investigated three-center XB complexes can be assigned to the increased polarizability in the O-X direction as compared to the direction of the initially most negative ESP of the halogen-bond acceptor. Therefore, although one could expect the σ-hole to interact with both oxygens equally in symmetric acceptors, the presence of positive potential (σ-hole) induces changes in the electron density and the asymmetric arrangement is formed. However no direct link between the geometry (orientation of dihalogen relative to the plane of aromatic system) and properties of XB acceptor was observed. This can be due to the fact that multiple minima can be found at the PES. A grid search of the PES might be necessary to shed light on this issue.

The nature of halogen bond in our model systems was studied by a vast number of methods including density-based as well as orbital-based methods. Our analyses suggest that the bifurcated halogen bonding (BXB) in current model systems benefit from both the electrostatic and exchange-correlation components and their contributions increase with increasing the interaction energy. It is worth mentioning that the exchange-correlation contribution, that is a manifestation of covalency, is the dominant factor for stabilizing weak halogen bonds. QTAIM analysis demonstrates that the delocalization index, a measure of electron exchange between neighboring atoms, for halogen-oxygen pairs correlates linearly with the binding energy. This linear correlation suggests that electron sharing increases uniformly by increasing the binding energy. This qualitative assumption was confirmed by quantitative Energy Decomposition Analysis. However, the relative contributions of the energy components change by changing the nature of the electron donor, i.e. changing the substituents on the benzene moiety. The exchange-correlation is the major contributor in the binding energy in positively charged complexes, whereas the contribution of the electrostatic forces surpasses that of the exchange-correlation and becomes the dominant factor in the complexes with negatively charged electron donors. The observations for the negatively charged systems can be rationalized by the less electron delocalization between the lone pairs of oxygens and π*-orbitals of the electron-rich aromatic ring

resulting in a more favorable interaction of LP-lumps at electron-rich oxygens with σ-hole of the dihalogen molecule. NBO analysis showed that by changing the orientation of the dihalogen molecules with respect to the XB acceptor, the contribution of different lone pairs of oxygens into the halogen bonding changes. Accordingly, depending on the orientation of the dihalogen molecule, this bifurcated interaction may be classified as 'σ-hole – lone pair' or 'σ-hole – π' bonding where σ-hole – LP denotes the interaction of XB donor with the lone pair oriented in the plane of the XB acceptor but σ-hole – π refers to the out-of-plane orientation.

Note added in revision

During the revision of this manuscript, a paper covering a similar topic (interaction of symmetric nitrogen-based XB donors with chlorine, bromine, and iodine molecules) from topological QTAIM and Interacting Quantum Atoms perspective was published.[74] The authors reported similar conclusions regarding the role of electrostatic and exchange in stabilizing the halogen bonds using a different approach.

ACKNOWLEDGMENT

This work was supported by the Czech Science Foundation (14-14654S to MN and RM) and carried out at CEITEC – the Central European Institute of Technology with research infrastructure supported by the project CZ.1.05/1.1.00/02.0068 financed by the European Regional Development Fund. C.F.-N. thanks the Program "Employment of Newly Graduated Doctors of Science for Scientific Excellence" (Grant Number CZ.1.07/2.3.00/30.009) co-financed by the European Social Fund and the state budget of the Czech Republic and the SoMoPro II program for partial support. The research leading to this invention has acquired a financial grant from the People Program (Marie Curie action) of the Seventh Framework Program of EU according to the REA Grant Agreement No. 291782. The research is further co-financed by the South-Moravian Region. Computational resources were provided by the MetaCentrum under the program LM2010005 and the CERIT-SC under the program Centre CERIT Scientific Cloud, part of the Operational Program Research and Development for Innovations, Reg. no. CZ.1.05/3.2.00/08.0144.

Electronic Supporting Information:

Table S1 and Table S2: Geometric properties of complexes with BrF. Table S3 and Table S4: QTAIM properties of complexes with BrF. Table S5 and Table S6: Geometric properties of complexes with ClF. Table S7 and Table S8: QTAIM properties of complexes with ClF. Table S9 and Table S10: Geometric properties of complexes with BrCl. Table S11 and Table S12: QTAIM properties of complexes with BrCl. Table S13: QTAIM properties of XB acceptors. Table S14 and Table S15: EDA analyses of selected complexes. Figure S1: Bonding and antibonding orbitals resulting from NOCV analysis along with $\Delta\rho_1$ electron deformation density.

REFERENCES

(1) Stone, A. *The Theory of Intermolecular Forces*; 2nd ed.; Oxford University Press, USA, 2013.

(2) Huber, S. M.; Scanlon, J. D.; Jimenez-Izal, E.; Ugalde, J. M.; Infante, I. On the Directionality of Halogen Bonding. *Phys. Chem. Chem. Phys.* **2013**, *15*, 10350–10357.

(3) Riley, K. E.; Murray, J. S.; Fanfrlík, J.; Řezáč, J.; Solá, R. J.; Concha, M. C.; Ramos, F. M.; Politzer, P. Halogen Bond Tunability I: The Effects of Aromatic Fluorine Substitution on the Strengths of Halogen-Bonding Interactions Involving Chlorine, Bromine, and Iodine. *J. Mol. Model.* **2011**, *17*, 3309–3318.

(4) Politzer, P.; Murray, J. S.; Clark, T. Halogen Bonding: An Electrostatically-Driven Highly Directional Noncovalent Interaction. *Phys. Chem. Chem. Phys.* **2010**, *12*, 7748–7757.

(5) Murray, J. S.; Lane, P.; Clark, T.; Riley, K. E.; Politzer, P. σ-Holes, π-Holes and Electrostatically-Driven Interactions. *J. Mol. Model.* **2012**, *18*, 541–548.

(6) Fanfrlík, J.; Kolář, M.; Kamlar, M.; Hurný, D.; Ruiz, F. X.; Cousido-siah, A.; Mitschler, A.; Řezáč, J.; Munusamy, E.; Lepšík, M.; Matějíček, P.; Veselý, J.; Podjarny, A.; Hobza, P. Modulation of Aldose Reductase Inhibition by Halogen Bond Tuning. *ACS Chem. Biol.* **2013**, *8*, 2484–2492.

(7) Wilcken, R.; Zimmermann, M. O.; Lange, A.; Joerger, A. C.; Boeckler, F. M. Principles and Applications of Halogen Bonding in Medicinal Chemistry and Chemical Biology. *J. Med. Chem.* **2013**, *56*, 1363–1388.

(8) Deepa, P.; Vijaya Pandiyan, B.; Kolandaivel, P.; Hobza, P. Halogen Bonds in Crystal TTF Derivatives: An Ab Initio Quantum Mechanical Study. *Phys. Chem. Chem. Phys.* **2014**, *16*, 2038–2047.

(9) Vener, M. V; Shishkina, A. V.; Rykounov, A. A.; Tsirelson, V. G. Cl···Cl Interactions in Molecular Crystals: Insights from the Theoretical Charge Density Analysis. *J. Phys. Chem. A* **2013**, *117*, 8459–8467.

(10) Tothadi, S.; Joseph, S.; Desiraju, G. R. Synthon Modularity in Cocrystals of 4-Bromobenzamide with N -Alkanedicarboxylic Acids: Type I and Type II Halogen···Halogen Interactions. *Cryst. Growth Des.* **2013**, *13*, 3242–3254.

(11) Ji, B.; Wang, W.; Deng, D.; Zhang, Y. Symmetrical Bifurcated Halogen Bond : Design and Synthesis. *Cryst. Growth Des.* **2011**, *11*, 3622–3628.

(12) Attrell, R. J.; Widdifield, C. M.; Korobkov, I.; Bryce, D. L. Weak Halogen Bonding in Solid Haloanilinium Halides Probed Directly via Chlorine-35, Bromine-81, and Iodine-127 NMR Spectroscopy. *Cryst. Growth Des.* **2012**, *12*, 1641–1653.

(13) Viger-Gravel, J.; Korobkov, I.; Bryce, D. L. Multinuclear Solid-State Magnetic Resonance and X-Ray Diffraction Study of Some Thiocyanate and Selenocyanate Complexes Exhibiting Halogen Bonding. *Cryst. Growth Des.* **2011**, *11*, 4984–4995.

(14) Bosch, E. Serendipity and the Search for Short N---I Halogen Bonds. *Cryst. Growth Des.* **2014**, *14*, 126–130.

(15) Clark, T. σ-Holes. *Wiley Interdiscip. Rev. Comput. Mol. Sci.* **2013**, *3*, 13–20.

(16) Politzer, P.; Riley, K. E.; Bulat, F. A.; Murray, J. S. Perspectives on Halogen Bonding and Other σ-Hole Interactions: Lex Parsimoniae (Occam's Razor). *Comput. Theor. Chem.* **2012**, *998*, 2–8.

(17) Esrafili, M. D. A Theoretical Investigation of the Characteristics of Hydrogen/Halogen Bonding Interactions in Dibromo-Nitroaniline. *J. Mol. Model.* **2013**, *19*, 1417–1427.

(18) Clark, T.; Hennemann, M.; Murray, J. S.; Politzer, P. Halogen Bonding: The Sigma-Hole. *J. Mol. Model.* **2007**, *13*, 291–296.

(19) Politzer, P.; Murray, J. S.; Clark, T. Halogen Bonding and Other σ-Hole Interactions: A Perspective. *Phys. Chem. Chem. Phys.* **2013**, *15*, 11178–11189.

(20) Politzer, P.; Murray, J. S. Halogen Bonding: An Interim Discussion. *ChemPhysChem* **2013**, *14*, 278–294.

(21) Politzer, P.; Murray, J. S.; Clark, T. σ-Hole Bonding: A Physical Interpretation. *Top. Curr. Chem.* **2014**.

(22) Voth, A. R.; Khuu, P.; Oishi, K.; Ho, P. S. Halogen Bonds as Orthogonal Molecular Interactions to Hydrogen Bonds. *Nat. Chem.* **2009**, *1*, 74–79.

(23) Bundhun, A.; Ramasami, P.; Murray, J. S.; Politzer, P. Trends in σ -Hole Strengths and Interactions of F3MX Molecules (M = C, Si, Ge and X = F, Cl, Br, I). *J. Mol. Model.* **2013**, *19*, 2739–2746.

(24) El-Sheshtawy, H. S.; Bassil, B. S.; Assaf, K. I.; Kortz, U.; Nau, W. M. Halogen Bonding inside a Molecular Container. *J. Am. Chem. Soc.* **2012**, *134*, 19935–19941.

(25) Amezaga, N. J. M.; Pamies, S. C.; Peruchena, N. M.; Sosa, G. L. Halogen Bonding: A Study Based on the Electronic Charge Density. *J. Phys. Chem. A* **2010**, *114*, 552–562.

(26) Duarte, D. J. R.; Sosa, G. L.; Peruchena, N. M. Nature of Halogen Bonding. A Study Based on the Topological Analysis of the Laplacian of the Electron Charge Density and an Energy Decomposition Analysis. *J. Mol. Model.* **2012**, *19*, 2035–2041.

(27) Dyduch, K.; Mitoraj, M. P.; Michalak, A. ETS-NOCV Description of σ-Hole Bonding. *J. Mol. Model.* **2013**, *19*, 2747–2758.

(28) Ding, X.; Tuikka, M.; Haukka, M. *Chapter 7 in Recent Advances in Crystallography*; Benedict, J. B., Ed.; InTech, **2012**.

(29) Eskandari, K.; Zariny, H. Halogen Bonding: A Lump–hole Interaction. *Chem. Phys. Lett.* **2010**, *492*, 9–13.

(30) Zhang, X.; Zeng, Y.; Li, X.; Meng, L.; Zheng, S. A Computational Study on the Nature of the Halogen Bond between Sulfides and Dihalogen Molecules. *Struct. Chem.* **2011**, *22*, 567–576.

(31) Riley, K. E.; Hobza, P. The Relative Roles of Electrostatics and Dispersion in the Stabilization of Halogen Bonds. *Phys. Chem. Chem. Phys.* **2013**, *15*, 17742–17751.

(32) Esrafili, M. D. Investigation of H-Bonding and Halogen-Bonding Effects in Dichloroacetic Acid: DFT Calculations of NQR Parameters and QTAIM Analysis. *J. Mol. Model.* **2012**, *18*, 5005–5016.

(33) Zou, J.-W.; Jiang, Y.-J.; Guo, M.; Hu, G.-X.; Zhang, B.; Liu, H.-C.; Yu, Q.-S. Ab Initio Study of the Complexes of Halogen-Containing Molecules RX (X=Cl, Br, and I) and NH3: Towards Understanding the Nature of Halogen Bonding and the Electron-Accepting Propensities of Covalently Bonded Halogen Atoms. *Chem. Eur. J.* **2005**, *11*, 740–751.

(34) Reed, A. E.; Curtiss, L. A.; Weinhold, F. Intermolecular Interactions from a Natural Bond Orbital, Donor-Acceptor Viewpoint. *Chem. Rev.* **1988**, *88*, 899–926.

(35) Li, R.; Li, Q.; Cheng, J.; Li, W. The Structure, Properties, and Nature of Unconventional π Halogen Bond in the Complexes of Al4(2-) and Halohydrocarbons. *J. Mol. Model.* **2012**, *18*, 2311–2319.

(36) Syzgantseva, O. A.; Tognetti, V.; Joubert, L. On the Physical Nature of Halogen Bonds: A QTAIM Study. *J. Phys. Chem. A* **2013**, *117*, 8969–8980.

(37) Riley, K. E.; Hobza, P. Investigations into the Nature of Halogen Bonding Including Symmetry Adapted Perturbation Theory Analyses. *J. Chem. Theory Comput.* **2008**, *4*, 232–242.

(38) Wolters, L. P.; Smits, N. W. G.; Fonseca Guerra, C. Covalency in Resonance-Assisted Halogen Bonds Demonstrated with Cooperativity in N-Halo-Guanine Quartets. *Phys. Chem. Chem. Phys.* **2015**, *17*, 1585–1592.

(39) Kolář, M.; Hobza, P. On Extension of the Current Biomolecular Empirical Force Field for the Description of Halogen Bonds. *J. Chem. Theory Comput.* **2012**, *8*, 1325–1333.

(40) El Hage, K.; Piquemal, J.-P.; Hobaika, Z.; Maroun, R. G.; Gresh, N. Could an Anisotropic Molecular Mechanics/dynamics Potential Account for Sigma Hole Effects in the Complexes of Halogenated Compounds? *J. Comput. Chem.* **2013**, *34*, 1125–1135.

(41) Kolář, M.; Hobza, P.; Bronowska, A. K. Plugging the Explicit σ-Holes in Molecular Docking. *Chem. Commun.* **2013**, *49*, 981–983.

(42) Eskandari, K.; Mahmoodabadi, N. Pnicogen Bonds: A Theoretical Study Based on the Laplacian of Electron Density. *J. Phys. Chem. A* **2013**, *117*, 13018–13024.

(43) Scheiner, S. The Pnicogen Bond: Its Relation to Hydrogen, Halogen, and Other Noncovalent Bonds. *Acc. Chem. Res.* **2013**, *46*, 280–288.

(44) An, X.-L.; Li, R.; Li, Q.-Z.; Liu, X.-F.; Li, W.-Z.; Cheng, J.-B. Substitution, Cooperative, and Solvent Effects on π Pnicogen Bonds in the FH(2)P and FH(2)As Complexes. *J. Mol. Model.* **2012**, *18*, 4325–4332.

(45) Murray, J. S.; Lane, P.; Clark, T.; Politzer, P. Sigma-Hole Bonding: Molecules Containing Group VI Atoms. *J. Mol. Model.* **2007**, *13*, 1033–1038.

(46) Thomas, S. P.; Pavan, M. S.; Guru Row, T. N. Experimental Evidence for "Carbon Bonding" in the Solid State from Charge Density Analysis. *Chem. Commun.* **2014**, *50*, 49–51.

(47) Lu, Y.-X.; Zou, J.-W.; Wang, Y.-H.; Yu, Q.-S. Bifurcated Halogen Bonds: An Ab Initio Study of the Three-Center Interactions. *J. Mol. Struct. THEOCHEM* **2006**, *767*, 139–142.

(48) Cinčić, D.; Friščić, T.; Jones, W. Experimental and Database Studies of Three-Centered Halogen Bonds with Bifurcated Acceptors Present in Molecular Crystals, Cocrystals and Salts. *CrystEngComm* **2011**, *13*, 3224.

(49) Frisch, M. J.; Trucks, G. W.; Schlegel, H. B.; Scuseria, G. E.; Robb, M. A.; Cheeseman, J. R.; Scalmani, G.; Barone, V.; Mennucci, B.; Petersson, G. A.; Nakatsuji, H.; Caricato, M.; Li, X.; Hratchian, H. P.; Izmaylov, A. F.; Bloino, J.; Zheng, G.; Sonnenberg, D. J.; Hada, M.; Ehara, M.; Toyota, K.; Fukuda, R.; Hasegawa, J.; Ishida, M.; Nakajima, T.; Honda, Y.; Kitao, O.; Nakai, H.; Vreven, T.; Montgomery, J. A. J.; Peralta, J. E.; Ogliaro, F.; Bearpark, M.; Heyd, J. J.; Brothers, E.; Kudin, K. N.; Staroverov, V. N.; Kobayashi, R.; Normand, J.; Raghavachari, K.; Rendell, A.; Burant, J. C.; Iyengar, S. S.; Tomasi, J.; Cossi, M.; Rega, N.; Millam, N. J.; Klene, M.; Knox, J. E.; Cross, J. B.; Bakken, V.; Adamo, C.; Jaramillo, J.; Gomperts, R.; Stratmann, R. E.; Yazyev, O.; Austin, A. J.; Cammi, R.; Pomelli, C.; Ochterski, J. W.; Martin, R. L.; Morokuma, K.; Zakrzewski, V. G.; Voth, G. A.; Salvador, P.; Dannenberg, J. J.; Dapprich, S.;

Daniels, A. D.; Farkas, Ö.; Foresman, J. B.; Ortiz, J. V.; Cioslowski, J.; Fox, D. J. Gaussian 09, Revision A2. *Gaussian*, **2009**.

(50) Zhao, Y.; Truhlar, D. G. The M06 Suite of Density Functionals for Main Group Thermochemistry, Thermochemical Kinetics, Noncovalent Interactions, Excited States, and Transition Elements: Two New Functionals and Systematic Testing of Four M06-Class Functionals and 12 Other Functionals. *Theor. Chem. Acc.* **2007**, *120*, 215–241.

(51) Kozuch, S.; Martin, J. M. L. Halogen Bonds: Benchmarks and Theoretical Analysis. *J. Chem. Theory Comput.* **2013**, *9*, 1918–1931.

(52) Rappoport, D.; Furche, F. Property-Optimized Gaussian Basis Sets for Molecular Response Calculations. *J. Chem. Phys.* **2010**, *133*, 134105.

(53) Glendening, E. D.; Reed, A. E.; Carpenter, J. E.; Weinhold, F. NBO Version 3.1.

(54) Bouzková, K.; Babinský, M.; Novosadová, L.; Marek, R. Intermolecular Interactions in Crystalline Theobromine as Reflected in Electron Deformation Density and 13 C NMR Chemical Shift Tensors. *J. Chem. Theory Comput.* **2013**, *9*, 2629–2638.

(55) Babinský, M.; Bouzková, K.; Pipíška, M.; Novosadová, L.; Marek, R. Interpretation of Crystal Effects on NMR Chemical Shift Tensors: Electron and Shielding Deformation Densities. *J. Phys. Chem. A* **2013**, *117*, 497–503.

(56) Baerends, E. J.; Ziegler, T.; Autschbach, J.; Bashford, D.; Bérces, A.; Bickelhaupt, F. M.; Bo, C.; Boerrigter, P. M.; Cavallo, L.; Chong, D. P.; Deng, L.; Dickson, R. M.; Ellis, D. E.; Faassen, M. van; Fan, L.; Fischer, T. H.; Guerra, C. F.; Ghysels, A.; Giammona, A.; Gisbergen, S. J. A. van; Götz, A. W.; Groeneveld, J. A.; Gritsenko, O. V.; Grüning, M.; Gusarov, S.; Harris, F. E.; Hoek, P. van den; Jacob, C. R.; Jacobsen, H.; Jensen, L.; Kaminski, J. W.; Kessel, G. van; Kootstra, F.; Kovalenko, A.; Krykunov, M. V.; Lenthe, E. van; McCormack, D. A.; Michalak, A.; Mitoraj, M.; Neugebauer, J.; Nicu, V. P.; Noodleman, L.; Osinga, V. P.; Patchkovskii, S.; Philipsen, P. H. T.; Post, D.; Pye, C. C.; Ravenek, W.; Rodríguez, J. I.; Ros, P.; Schipper, P. R. T.; Schreckenbach, G.; Seldenthuis, J. S.; Seth, M.; Snijders, J. G.; Solà, M.; Swart, M.; Swerhone, D.; Te Velde, G.; Vernooijs, P.; Versluis, L.; Visscher, L.; Visser, O.; Wang, F.; Wesolowski, T. A.; Wezenbeek, E. M. van; Wiesenekker, G.; Wolff, S. K.; Woo, T. K.; Yakovlev, A. L. ADF2013, SCM, Theoretical Chemistry, Vrije Universiteit, Amsterdam, The Netherlands.

(57) Te Velde, G.; Bickelhaupt, F. M.; Baerends, E. J.; Guerra, C. F.; van Gisbergen, S. J. A.; Snijders, J. G.; Ziegler, T. Chemistry with ADF. *J. Comput. Chem.* **2001**, *22*, 931–967.

(58) Mitoraj, M.; Michalak, A. Natural Orbitals for Chemical Valence as Descriptors of Chemical Bonding in Transition Metal Complexes. *J. Mol. Model.* **2007**, *13*, 347–355.

(59) Mitoraj, M. P.; Michalak, A.; Ziegler, T. A Combined Charge and Energy Decomposition Scheme for Bond Analysis. *J. Chem. Theory Comput.* **2009**, *5*, 962–975.

(60) Bader, R. W. F. *Atoms in Molecules. A Quantum Theory*; Clarendon: Oxford, U.K., **1990**.

(61) Keith, T. A. AIMAll (Version 13.11.04), **2013**.

(62) Desiraju, G. R.; Ho, P. S.; Kloo, L.; Legon, A. C.; Marquardt, R.; Metrangolo, P.; Politzer, P.; Resnati, G.; Rissanen, K. Definition of the Halogen Bond (IUPAC Recommendations 2013). *Pure Appl. Chem.* **2013**, *85*, 1711–1713.

(63) Clark, T.; Politzer, P.; Murray, J. S. Correct Electrostatic Treatment of Noncovalent Interactions: The Importance of Polarization. *Wiley Interdiscip. Rev. Comput. Mol. Sci.* **2015**, DOI: 10.1002/wcms.1210.

(64) Foroutan-Nejad, C.; Shahbazian, S.; Marek, R. Toward a Consistent Interpretation of the QTAIM: Tortuous Link between Chemical Bonds, Interactions, and Bond/line Paths. *Chem. Eur. J.* **2014**, *20*, 10140–10152.

(65) Bader, R. W. F.; Stephens, M. E. Spatial Localization of the Electronic Pair and Number Distributions in Molecules. *J. Am. Chem. Soc.* **1975**, *97*, 7391–7399.

(66) Cortesguzman, F.; Bader, R. Complementarity of QTAIM and MO Theory in the Study of Bonding in Donor-Acceptor Complexes. *Coord. Chem. Rev.* **2005**, *249*, 633–662.

(67) Pendás, Á. M.; Blanco, M. A.; Francisco, E. Two-Electron Integrations in the Quantum Theory of Atoms in Molecules. *J. Chem. Phys.* **2004**, *120*, 4581–4592.

(68) Blanco, M. A.; Pendás, Á. M.; Francisco, E. Interacting Quantum Atoms: A Correlated Energy Decomposition Scheme Based on the Quantum Theory of Atoms in Molecules. *J. Chem. Theory Comput.* **2005**, *1*, 1096–1109.

(69) Kitaura, K.; Morokuma, K. A New Energy Decomposition Scheme for Molecular Interactions within the Hartree-Fock Approximation. *Int. J. Quantum Chem.* **1976**, *10*, 325–340.

(70) Ziegler, T.; Rauk, A. A Theoretical Study of the Ethylene-Metal Bond in Complexes between copper(1+), silver(1+), gold(1+), platinum(0) or platinum(2+) and Ethylene, Based on the Hartree-Fock-Slater Transition-State Method. *Inorg. Chem.* **1979**, *1979*, 1558–1565.

(71) García-Revilla, M.; Francisco, E.; Popelier, P. L. A.; Pendás, Á. M. Domain-Averaged Exchange-Correlation Energies as a Physical Underpinning for Chemical Graphs. *ChemPhysChem* **2013**, *14*, 1211–1218.

(72) Poater, J.; Solà, M.; Bickelhaupt, F. M. Hydrogen-Hydrogen Bonding in Planar Biphenyl, Predicted by Atoms-in-Molecules Theory, Does Not Exist. *Chem. Eur. J.* **2006**, *12*, 2889–2895.

(73) Toušek, J.; Straka, M.; Sklenář, V.; Marek, R. Origin of the Conformational Modulation of the 13C NMR Chemical Shift of Methoxy Groups in Aromatic Natural Compounds. *J. Phys. Chem. A* **2013**, *117*, 661–669.

(74) Bartashevich, E.; Troitskaya, E.; Pendás, Á. M.; Tsirelson, V. Understanding the Bifurcated Halogen Bonding N···Hal···N in Bidentate Diazaheterocyclic Compounds. *Comput. Theor. Chem.* **2015**, *1053*, 229–237.